



Analyzing local Lorentz violation with gravitational experiments

ChengGang Shao, Ya-Fen Chen, and Yu-Jie Tan

Center for Gravitational Experiment (CGE),
Huazhong University of Science and Technology (HUST),
Wuhan, China

2017.09.24 Corfu2017

Outline

- Lorentz violation in the gravitational sector
- Limits on Lorentz violation from gravimeters and tests of the gravitational inverse square law
- Recent experimental design for Lorentz violation in short-range gravity

I. Lorentz violation in the gravitational sector

Gravitational phenomena ←

GR ← Einstein Equivalence Principle (three logical parts):

Weak equivalence principle (**WEP**), has been widely tested

Local Lorentz invariance (**LLI**), tested for many sectors of the SM

Local Position invariance (**LPI**), also no violation

- Lorentz violation in gravity

Lorentz violation ---- Described by the presence of **background general tensor fields** in spacetime $(s_{\mu\nu}, k_{\mu\nu\kappa\lambda}, \dots)$

The topic :

How to constrain LV from laboratory gravitational experiments and how to design experiments to improve constraints of LV?

Theoretical model of LV in gravity



General framework: **Standard-Model Extension (SME)**
(developed by Kostelecky and collaborators)

Lagrangian of LV in **gravity**

$$L_{\text{LV}} = \frac{\sqrt{g}}{16\pi G} (L_{\text{LV}}^{(4)} + L_{\text{LV}}^{(5)} + L_{\text{LV}}^{(6)} + \dots) \quad \text{Bailey, PRD91,022006(2015)}$$

a series involving operators of increasing mass dimension d

$L_{\text{LV}}^{(4)}$ ← **Tested by interaction between Earth and a small test body.**

$L_{\text{LV}}^{(5)}$ has no effect on nonrelativistic gravity

$L_{\text{LV}}^{(6)}$ ← **Tested in short-range gravity.**

minimal SME (mSME)



The minimal term with $d = 4$

$$L_{LV}^{(4)} = (k^{(4)})_{\alpha\beta\gamma\delta} R^{\alpha\beta\gamma\delta}$$

The dimensionless coefficient

trace ↓

$$-uR + s^{\mu\nu} R_{\mu\nu} + t^{\kappa\lambda\mu\nu} R_{\kappa\lambda\mu\nu}$$

- Atom-interferometer
- Lunar laser ranging
- Pulsar-timing observations

$$V(r) = -G \frac{m_1 m_2}{|\vec{x}_1 - \vec{x}_2|} \left[1 + \frac{1}{2} \hat{x}^j \hat{x}^k \bar{s}_{jk} \right]$$

9 independent components $\bar{s}^{\mu\nu} \square 10^{-10}$

Laboratory experiments: To measure the acceleration of a free body

Due to the Earth's orbit and rotation

$$\text{the local acceleration for LV } \frac{g_{LV}}{g} \propto \sum_m C_m \cos \omega_m t + D_m \sin \omega_m t$$

$$\text{Six frequencies } \omega_m = (2\omega_{\oplus}, \omega_{\oplus}, 2\omega_{\oplus} + \Omega, 2\omega_{\oplus} - \Omega, \omega_{\oplus} + \Omega, \omega_{\oplus} - \Omega)$$

Non-minimal term with $d = 6$



LV in short-range gravity.

Bailey, PRD91,022006(2015)

Lagrangian includes quadratic couplings of Riemann curvature

$$L_{\text{LV}}^{(6)} = \frac{1}{2} (k_1^{(6)})_{\alpha\beta\gamma\delta\kappa\lambda} \{D^\kappa, D^\lambda\} R^{\alpha\beta\gamma\delta} + (k_2^{(6)})_{\alpha\beta\gamma\delta\kappa\lambda\mu\nu} R^{\alpha\beta\gamma\delta} R^{\kappa\lambda\mu\nu}$$

Nonrelativistic effects
in post-Newtonian gravity

LV is described by the
effective coefficients

$$(\bar{k}_{\text{eff}})_{jklm}$$

Totally symmetric indices \rightarrow 15 independent coefficients

$$\text{Modified Poisson equation } \nabla^2 U + 4\pi G \rho(\vec{r}) + (\bar{k}_{\text{eff}})_{jklm} \partial_j \partial_k \partial_l \partial_m U = 0$$

$$\text{In the case of two point masses } V(r) = -G \frac{m_1 m_2}{r} \left[1 + \frac{\bar{k}(\hat{r})}{r^2} \right]$$

Potential between two point masses



$$V_{LV}(\vec{r}) = -Gm_1m_2 \frac{\bar{k}(\hat{r})}{r^3} \quad r = |\vec{x}_1 - \vec{x}_2|$$

anisotropic combination of coefficients $(\bar{k}_{eff})_{ijkl}$,
function of \hat{r} direction

Bailey, PRD91,022006(2015)

$$\bar{k}(\hat{r}) = \frac{3}{2}(\bar{k}_{eff})_{ijij} - 9(\bar{k}_{eff})_{ijkk} \hat{r}^i \hat{r}^j + \frac{15}{2}(\bar{k}_{eff})_{ijkl} \hat{r}^i \hat{r}^j \hat{r}^k \hat{r}^l$$

Compare to usual Yukawa potential

$$V_{Yuk}(r) = -Gm_1m_2 \frac{\alpha e^{-r/\lambda}}{r}$$

Distinctive feature of LV : anisotropic cubic potential

depends on sidereal time in lab frame

Tests in short-range gravity

- constrain Yukawa parameter (α, λ)
- constrain Lorentz violation $(\bar{k}_{eff})_{jklm}$

II. Limits on Lorentz violation from gravimeters and tests of the gravitational inverse square law

Current lab test for minimal term d=4: Gravimeter

Such as atom-interferometer or superconductor gravimeter

Vertical acceleration

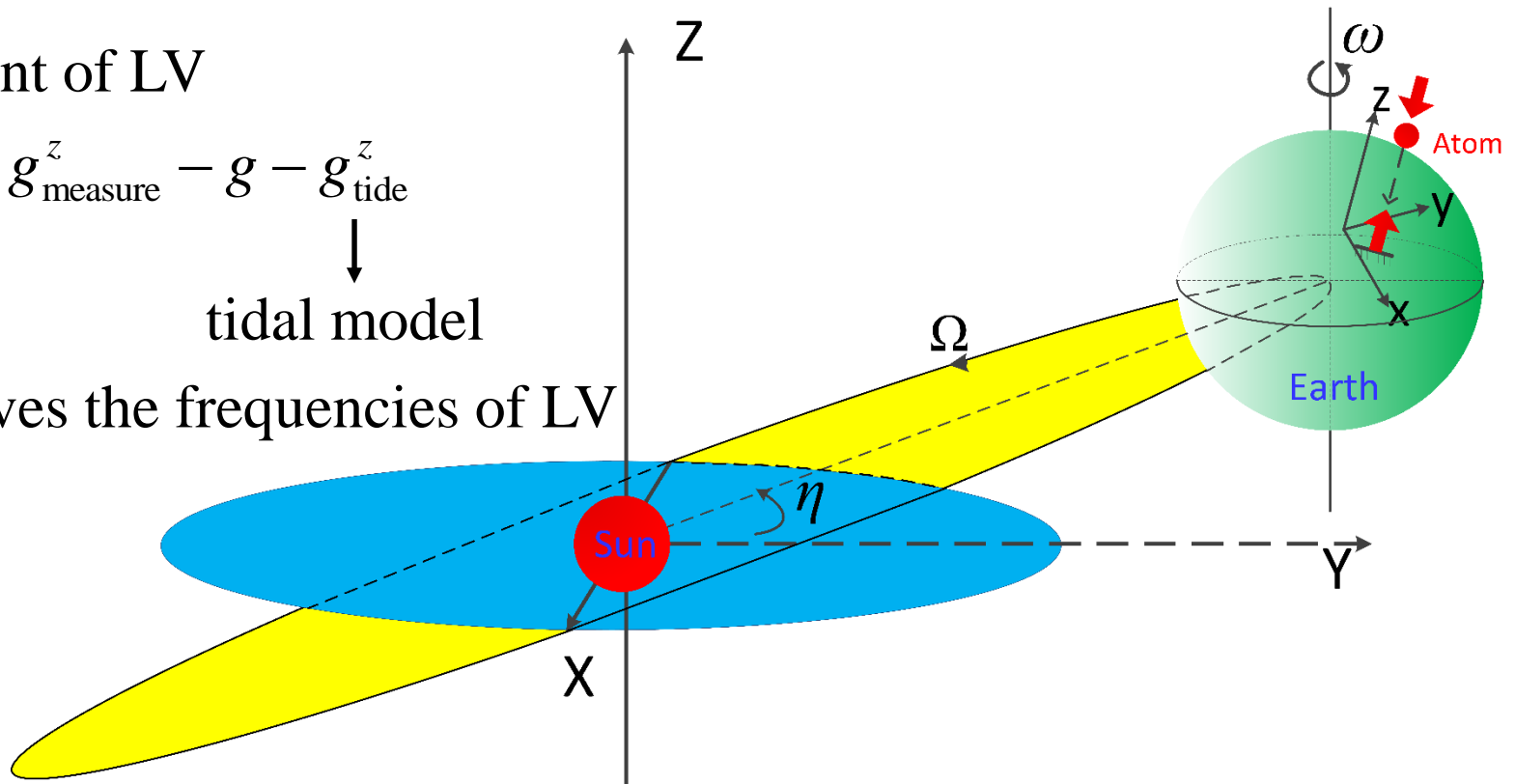
$$g_{\text{measure}}^z = g + g_{LV}^z + g_{\text{tide}}^z \quad \text{tidal effect}$$

Constraint of LV

$$g_{LV}^z = g_{\text{measure}}^z - g - g_{\text{tide}}^z$$

tidal model

involves the frequencies of LV



Theory of Lorentz violation analysis with tidal data

Data analysis

Superconducting-Gravimeter data

$$\delta g = g_{\text{measure}} - \boxed{g_{\text{tide model}}}$$

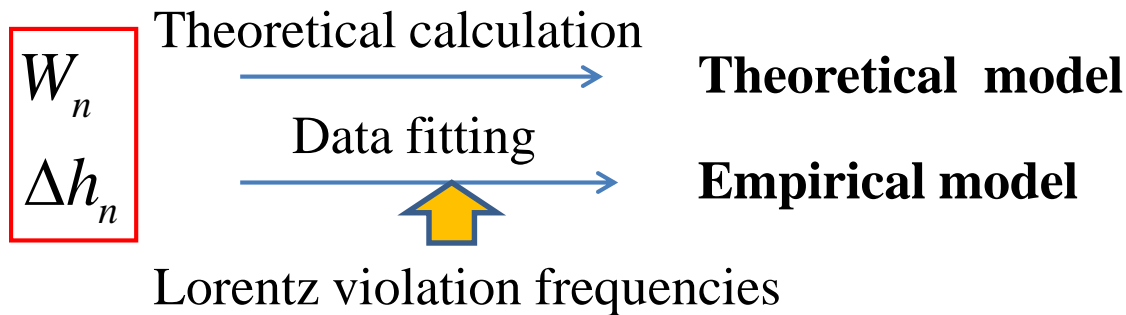
$$\frac{\delta g}{g_0} = \sum_m C_m \cos(\omega_m t + \phi_m) + D_m (\sin \omega_m t + \phi_m)$$

$\overline{S}^{\mu\nu}$

Tidal model

$$G_{\text{theory}}(t) = \sum_{n=1}^p W_n \cdot \sum_{k=n_i}^{n_f} H_k \cos(\omega_k t + h_k + \Delta h_n)$$

superposition of different wave groups



$$g_{\text{tide model}} = G_{\text{theory}} - \text{Ocean Loading correction} + \text{pressure correction}$$

LV from worldwide superconducting gravimeters

The constraints for LV coefficients are limited by the precision of tidal model

Combined result for 12 stations data

C.G.Shao. et al, arXiv: 1707.02318v1

Example

Medicina, Italy (-5.7152).

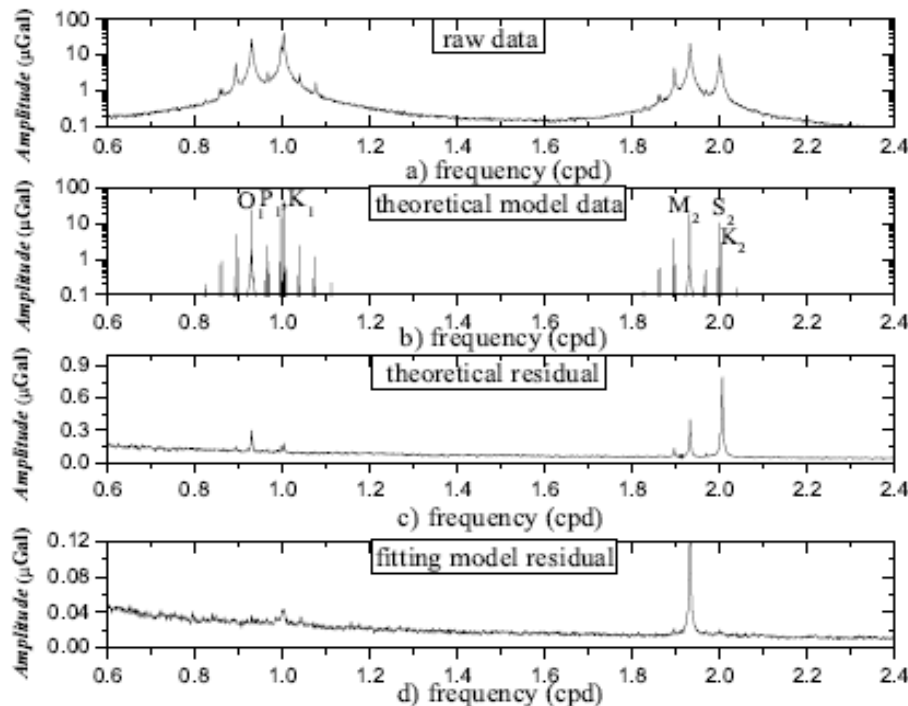


TABLE III: The comparison of Lorentz violation (LV) bounds from atom interferometry [11], the superconducting gravimeter at Bad Homburg [13] and a worldwide array of superconducting gravimeters in this work. This is the first bound of Lorentz violation obtained by a first-principles tidal model with ocean tides. The possible systematic error given here is based on residual spectrum at 2ω .

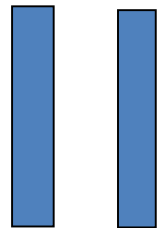
Coefficient	Atom interferometry [11]	Superconducting gravimeter at Bad Homburg [13]	LV estimate with statistical errors	LV systematic errors from the tidal model	Overall estimate of LV in this work
$\bar{s}^{XX} - \bar{s}^{YY}$	$(4.4 \pm 11) \times 10^{-9}$	$(2 \pm 1) \times 10^{-10}$	$(-8.8 \pm 0.5) \times 10^{-10}$	2.4×10^{-9}	$(-0.9 \pm 2.4) \times 10^{-9}$
\bar{s}^{XY}	$(0.2 \pm 3.9) \times 10^{-9}$	$(-4 \pm 1) \times 10^{-10}$	$(-11.0 \pm 0.3) \times 10^{-10}$	1.2×10^{-9}	$(-1.1 \pm 1.2) \times 10^{-9}$
\bar{s}^{XZ}	$(-2.6 \pm 4.4) \times 10^{-9}$	$(0 \pm 1) \times 10^{-10}$	$(-3.0 \pm 1.4) \times 10^{-11}$	1.8×10^{-10}	$(-0.3 \pm 1.8) \times 10^{-10}$
\bar{s}^{YZ}	$(-0.3 \pm 4.5) \times 10^{-9}$	$(3 \pm 1) \times 10^{-10}$	$(-2.4 \pm 1.4) \times 10^{-11}$	1.8×10^{-10}	$(-0.2 \pm 1.8) \times 10^{-10}$

Current test for non-minimal term $d=6$: test of ISL

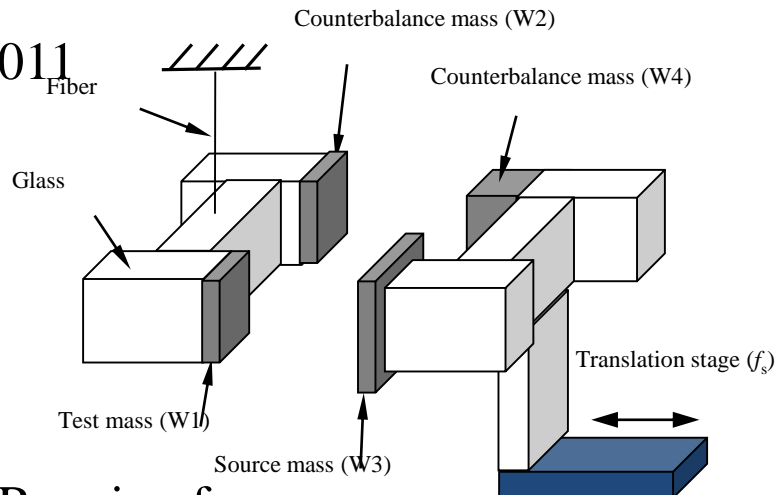


ISL Experiment, HUST-2011

PRL 108,081101(2012)



plane-to-plane
Geometry

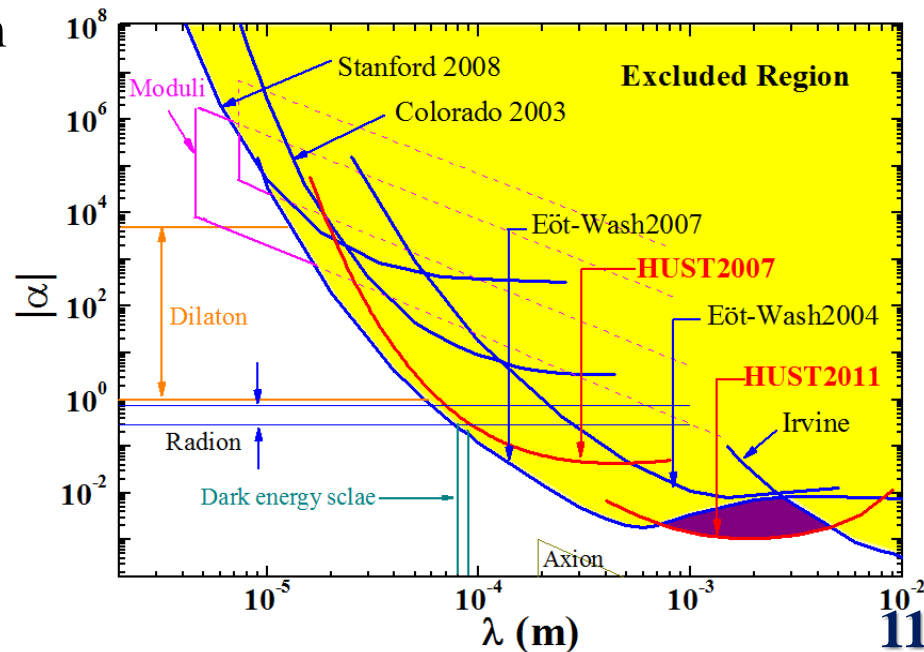


Ranging from
0.4 to 1.0 mm

Basic feature: I-shaped pendulum

Source mass platform: facing the
pendulum, I-shaped structure

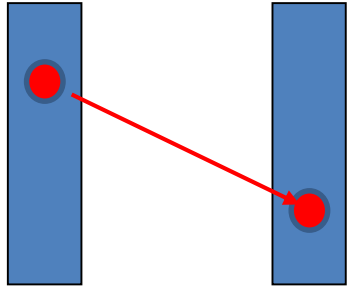
The separation was modulated by
driving a motor translation stage



LV($d=6$) in short-range gravity



Potential between two point masses



$$V_{LV}(r) \equiv -G \frac{m_1 m_2}{r^3} \bar{k}(\hat{r}) \quad r = |\vec{x}_1 - \vec{x}_2|$$

$$\bar{k}(\hat{r}) = \frac{3}{2} (\bar{k}_{eff})_{ijij} - 9 (\bar{k}_{eff})_{ijkk} \hat{r}^i \hat{r}^j + \frac{15}{2} (\bar{k}_{eff})_{ijkl} \hat{r}^i \hat{r}^j \hat{r}^k \hat{r}^l$$

Sidereal Time T-dependent

$$(\bar{k}_{eff})_{jklm} = R^{jJ} R^{kK} R^{lL} R^{mM} (\bar{k}_{eff})_{JKLM}$$

Laboratory frame

Sun-centered frame

χ : colatitude of the lab $\omega_{\oplus} \square 2\pi / 23\text{h}56\text{min}$

$$R^{jJ} = \begin{pmatrix} \cos \chi \cos \omega_{\oplus} T & \cos \chi \sin \omega_{\oplus} T & -\sin \chi \\ -\sin \omega_{\oplus} T & \cos \omega_{\oplus} T & 0 \\ \sin \chi \cos \omega_{\oplus} T & \sin \chi \sin \omega_{\oplus} T & \cos \chi \end{pmatrix}$$

Earth's sidereal Frequency

In laboratory frame

$$\bar{k}(\hat{r}, T) = c_0 + \sum_{m=1}^4 (c_m \cos m\omega_{\oplus} T + s_m \sin m\omega_{\oplus} T)$$

up to and including the fourth harmonic

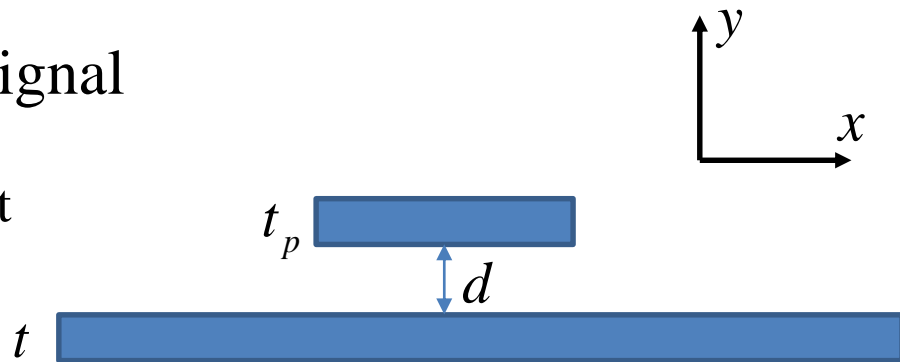
LV force between two plates

Planar geometry: to suppress the Newtonian background

However, it also suppresses the LV signal

$$F_{Newton}^y(d)|_{infinite} = \text{constant}$$

$$F_{LV}^y(d)|_{infinite} = 0$$



Force between two finite plates is dominated by the edge effect.

$$\Delta F_{LV}^y = F_{LV}^y(d_{min}) - F_{LV}^y(d_{max}) \sim \varepsilon \Delta C (\bar{k}_{eff})_{jkjk}$$

$$\Delta C \equiv 2\pi G \rho_p \rho A_p \left[\ln \frac{(d_{min} + t_p)(d_{min} + t)}{(d_{min} + t_p + t)d_{min}} - \ln \frac{(d_{max} + t_p)(d_{max} + t)}{(d_{max} + t_p + t)d_{max}} \right]$$

HUST-2011



dimensionless parameter ε : edge effect

Edge effect ε is typically of order ~ 0.01 or d / \sqrt{A}

Experimental result of LV in HUST-2011

$\tau_{measured}^z(t) = \tau_{LV}(T) \cos(2\pi f_s t + \varphi)$ LV torque was modulated by changing d

$$\tau_{LV}(T) = C_0 + \sum_{m=1}^4 [C_m \cos(m\omega_{\oplus} T) + S_m \sin(m\omega_{\oplus} T)]$$

	10^{-16}Nm
C_0	-0.22 ± 0.95
C_1	0.13 ± 0.22
S_1	-0.40 ± 0.23
C_2	-0.04 ± 0.22
S_2	0.20 ± 0.22
C_3	-0.30 ± 0.22
S_3	-0.25 ± 0.23
C_4	-0.06 ± 0.23
S_4	0.05 ± 0.23

	Keff	10^{-8}m^2
1	XXXX	-0.2 ± 2.8
2	YYYY	0.4 ± 2.8
3	ZZZZ	-0.9 ± 7.7
4	XXXY	0.4 ± 1.3
5	XXXZ	-0.1 ± 0.5
6	YYYX	0.6 ± 1.3
7	YYYZ	-0.4 ± 0.5
8	ZZZX	-1.3 ± 1.4
9	ZZZY	-0.2 ± 1.3
10	XXYY	-0.1 ± 1.7
11	XXZZ	-0.2 ± 1.0
12	YYZZ	0.2 ± 1.0
13	XXYZ	0.5 ± 0.5
14	YYXZ	-0.2 ± 0.5
15	ZZXY	-0.2 ± 0.5

$16 \times 16 \times 1.8 \text{ mm}^3$



$21 \times 21 \times 1.8 \text{ mm}^3$



Area

C.G. Shao, et.al.
PRD91, 102007 (2015)

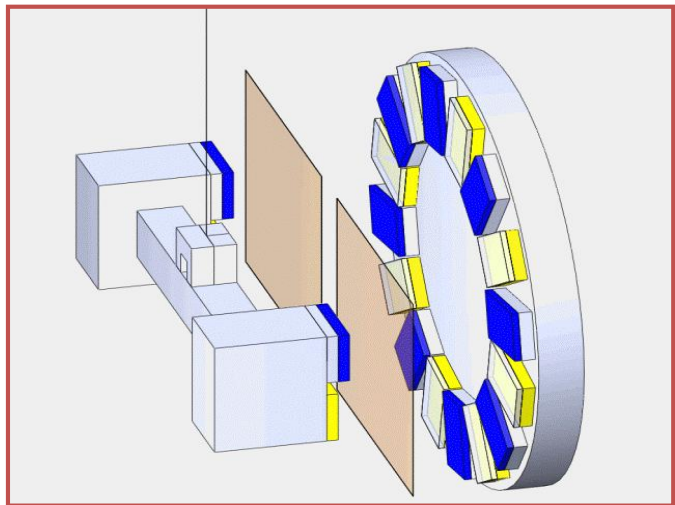
Each constraint of $(\bar{k}_{eff})_{JKLM}$ was obtained in turn by setting the other 14 degrees of freedom to be zero.

J.C. Long, et.al.
PRD91, 092003 (2015)

Our result: similar to that of IU-2002,2012, a shorter range ISL experiment ($80\mu\text{m}$)

ISL Experiment in HUST-2015

HUST-2015 separation: 0.295 mm

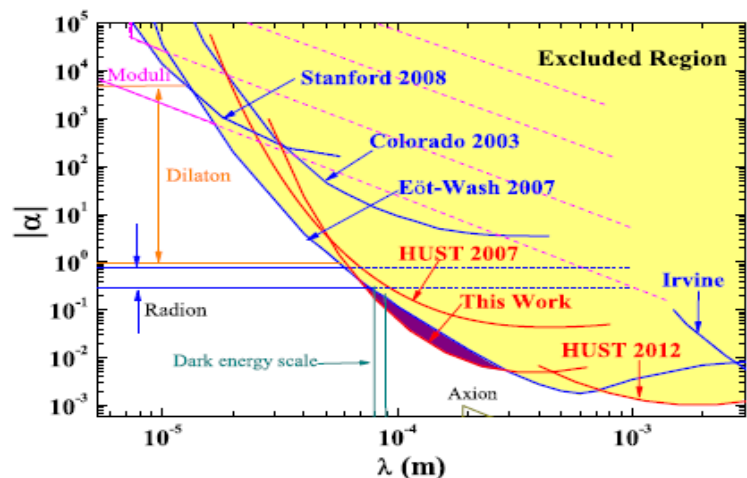


Combined analysis for HUST-2015, HUST-2011, IU-2012, IU-2002

TABLE II. Independent coefficient values (2σ , units 10^{-9} m^2) obtained by combining HUST and IU data [8–10].

Coefficient	Measurement
$(\bar{k}_{\text{eff}})_{XXXX}$	6.4 ± 32.9
$(\bar{k}_{\text{eff}})_{XXXY}$	0.0 ± 8.1
$(\bar{k}_{\text{eff}})_{XXXZ}$	-2.0 ± 2.6
$(\bar{k}_{\text{eff}})_{XXYY}$	-0.9 ± 10.9
$(\bar{k}_{\text{eff}})_{XXYZ}$	1.1 ± 1.2
$(\bar{k}_{\text{eff}})_{XXZZ}$	-2.6 ± 17.1
$(\bar{k}_{\text{eff}})_{XYYY}$	3.9 ± 8.1
$(\bar{k}_{\text{eff}})_{XYYZ}$	-0.6 ± 1.2
$(\bar{k}_{\text{eff}})_{XYZZ}$	-1.0 ± 1.0
$(\bar{k}_{\text{eff}})_{XZZZ}$	-8.1 ± 10.3
$(\bar{k}_{\text{eff}})_{YYYY}$	7.0 ± 32.9
$(\bar{k}_{\text{eff}})_{YYYZ}$	0.3 ± 2.6
$(\bar{k}_{\text{eff}})_{YYZZ}$	-2.5 ± 17.1
$(\bar{k}_{\text{eff}})_{YZZZ}$	3.6 ± 10.2

Improved the constraint of Yukawa parameter by a factor of 2.



Shao et.al, PRL117,071102(2016)

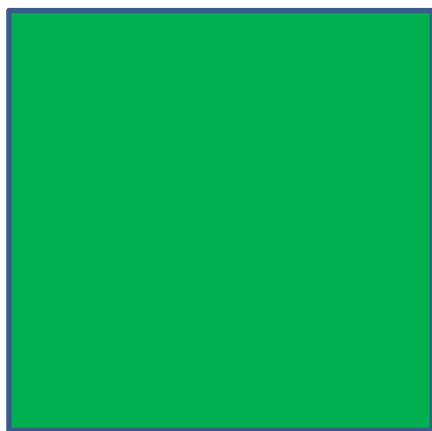
Tan et.al, PRL116,031101(2016)

III. Recent experimental design for Lorentz violation in short-range gravity

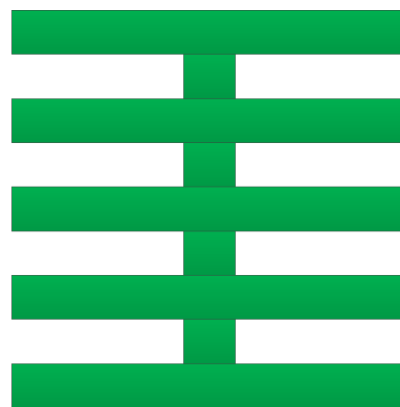


- Almost all experiments on ISL adopt planar geometry to search for Yukawa-type non-Newton gravity, which also suppressed LV signal
- LV force between two finite flat plates is dominated by edge effect

Our intuition tell us: plate with striped or checkered pattern



homogeneous-plate

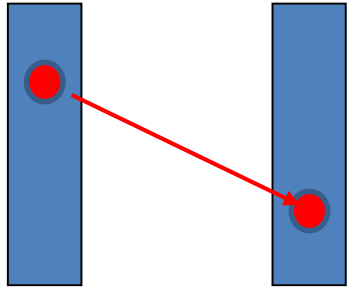


striped pattern



14 measurable independently coefficients of LV

Double trace of $(\bar{k}_{eff})_{ijij}$ is a rotational scalar, and can't be measured in short-range gravity



Measured LV torque provides nine components

$$\tau_{LV} = C_0 + \sum_{m=1}^4 C_m \cos(m\omega_{\oplus}T) + S_m \sin(m\omega_{\oplus}T)$$

Equivalently, $\bar{k}(\hat{r}) = c_0 + \sum_{m=1}^4 c_m \cos(m\omega_{\oplus}T) + s_m \sin(m\omega_{\oplus}T)$

Nine components in $\bar{k}(\hat{r})$ are functions of the 14 constant coefficients (\bar{k}_{eff}) in Sun-centered frame.

14 measurable coefficients can be redefined by excluding the unmeasurable degree of freedom

A spherical decomposition



A convenient formalism for analyzing short-range test of LV

Lagrange density $L = L_0 + L_{LV} = L_0 + \frac{1}{4} h_{\mu\nu} (\hat{s}^{\mu\rho\nu\sigma} + \hat{q}^{\mu\rho\nu\sigma} + \hat{k}^{\mu\nu\rho\sigma}) h_{\rho\sigma}$

V. A. Kostelecky. et al, PLB766,137-143(2017)

Cartesian coordinate system \longleftrightarrow spherical coordinate system

$\bar{k}(\hat{r}, T) = \sum_{jm} Y_{jm}(\theta, \phi) k_{jm}^{N(d)lab} \Rightarrow$ **Lorentz violation coefficients**

$k_{jm}^{N(d)lab} = \sum_{m'} e^{im\varphi} e^{im'\omega_{\oplus}T} d_{mm'}^{(j)}(-\chi) k_{jm'}^{N(d)}$

Lab frame \uparrow Sun-centered frame

$\left\{ \begin{array}{l} j = d - 2 \text{ or } d - 4 \\ m = -j, \dots, j \end{array} \right. \Rightarrow \left\{ \begin{array}{l} \text{Re } k_{jm}^{N(d)} \\ \text{Im } k_{jm}^{N(d)} \end{array} \right.$

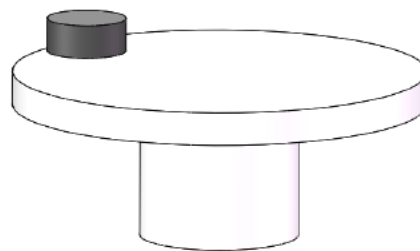
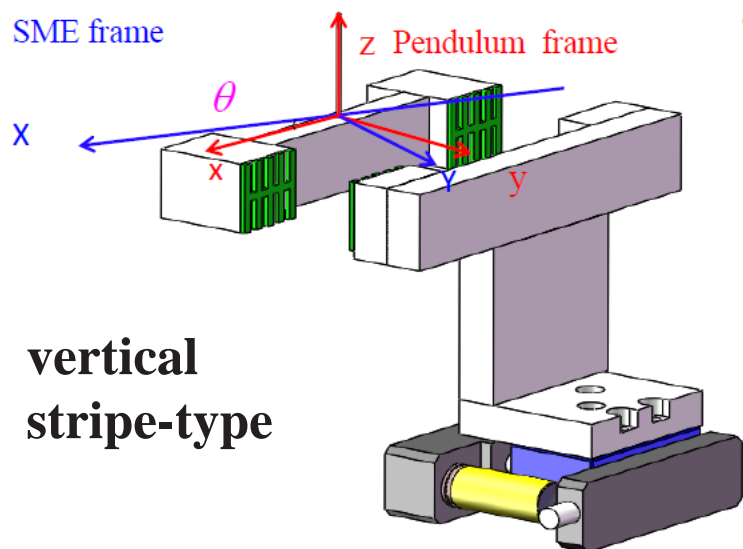
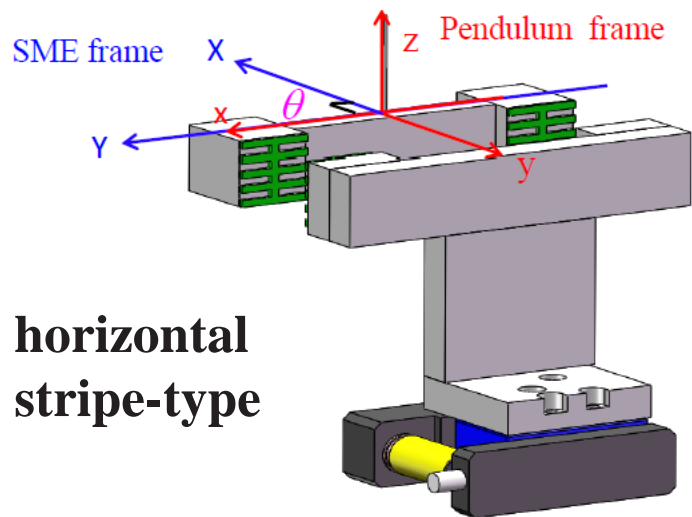
The spherical decomposition provide a clean separation of the observable harmonics in sidereal time.

Transformation matrix(d=6)

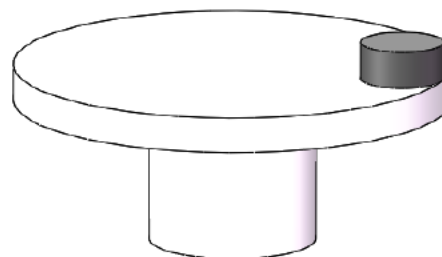
Newton spherical coefficients \longleftrightarrow Effective Cartesian coefficients

$$\begin{bmatrix} k_{2,0} \\ \text{Re}k_{2,1} \\ \text{Im}k_{2,-1} \\ \text{Re}k_{2,2} \\ \text{Im}k_{2,-2} \\ k_{4,0} \\ \text{Re}k_{4,1} \\ \text{Im}k_{4,-1} \\ \text{Re}k_{4,2} \\ \text{Im}k_{4,-2} \\ \text{Re}k_{4,3} \\ \text{Im}k_{4,-3} \\ \text{Re}k_{4,4} \\ \text{Im}k_{4,-4} \end{bmatrix} = \frac{\sqrt{\pi}}{7} \begin{bmatrix} 36/\sqrt{5} & 0 & 0 & 72/\sqrt{5} & 0 & 36/\sqrt{5} & 0 & 0 & 0 & 0 & 0 & 36/\sqrt{5} & 0 & 36/\sqrt{5} & 0 \\ 0 & 0 & 12\sqrt{6/5} & 0 & 0 & 0 & 0 & 12\sqrt{6/5} & 0 & 12\sqrt{6/5} & 0 & 0 & 0 & 0 & 0 \\ 0 & 0 & 0 & 0 & -12\sqrt{6/5} & 0 & 0 & 0 & 0 & 0 & 0 & -12\sqrt{6/5} & 0 & -12\sqrt{6/5} & 0 \\ -6\sqrt{6/5} & 0 & 0 & 0 & 0 & 6\sqrt{6/5} & 0 & 0 & 0 & 0 & 6\sqrt{6/5} & 0 & 6\sqrt{6/5} & 0 & 0 \\ 0 & 12\sqrt{6/5} & 0 & 0 & 0 & 0 & 12\sqrt{6/5} & 0 & 12\sqrt{6/5} & 0 & 0 & 0 & 0 & 0 & 0 \\ -5 & 0 & 0 & -10 & 0 & -40\sqrt{10} & 0 & 0 & 0 & 0 & -5 & 0 & -40 & 0 & 0 \\ 0 & 0 & 6 & 0 & 0 & 0 & 6\sqrt{5} & 0 & -8\sqrt{5} & 0 & 0 & 0 & 0 & 0 & 0 \\ 0 & 0 & 0 & 0 & -6\sqrt{5} & 0 & 0 & 0 & 0 & 0 & 0 & -6\sqrt{5} & 0 & 8\sqrt{5} & 0 \\ -\sqrt{10} & 0 & 0 & 0 & 0 & -10\sqrt{5} & 0 & 0 & 0 & 0 & \sqrt{10} & 0 & -6\sqrt{10} & 0 & 0 \\ 0 & 2\sqrt{10} & 0 & 0 & 0 & 0 & 2\sqrt{10} & 0 & -12\sqrt{10} & 0 & 0 & 0 & 0 & 0 & 0 \\ 0 & 0 & -2\sqrt{35} & 0 & 0 & 0 & 0 & 6\sqrt{35} & 0 & 0 & 0 & 0 & 0 & 0 & 0 \\ 0 & 0 & 0 & 0 & 6\sqrt{35} & 0 & 0 & 0 & 0 & 0 & 0 & -2\sqrt{35} & 0 & 0 & 0 \\ \sqrt{5/2} & 0 & 0 & -3\sqrt{70} & 0 & 0 & 0 & 0 & 0 & 0 & \sqrt{5/2} & 0 & 0 & 0 & 0 \\ 0 & -2\sqrt{70} & 0 & 0 & 0 & 0 & 2\sqrt{70} & 0 & 0 & 0 & 0 & 0 & 0 & 0 & 0 \end{bmatrix} \begin{bmatrix} (\bar{k}_{\text{eff}})_{\text{XXXX}} \\ (\bar{k}_{\text{eff}})_{\text{XXXY}} \\ (\bar{k}_{\text{eff}})_{\text{XXXZ}} \\ (\bar{k}_{\text{eff}})_{\text{XXYY}} \\ (\bar{k}_{\text{eff}})_{\text{XXYZ}} \\ (\bar{k}_{\text{eff}})_{\text{XXZZ}} \\ (\bar{k}_{\text{eff}})_{\text{XYYY}} \\ (\bar{k}_{\text{eff}})_{\text{XYYZ}} \\ (\bar{k}_{\text{eff}})_{\text{XYYZ}} \\ (\bar{k}_{\text{eff}})_{\text{XZZZ}} \\ (\bar{k}_{\text{eff}})_{\text{YYYY}} \\ (\bar{k}_{\text{eff}})_{\text{YYYY}} \\ (\bar{k}_{\text{eff}})_{\text{YYYZ}} \\ (\bar{k}_{\text{eff}})_{\text{YYZZ}} \\ (\bar{k}_{\text{eff}})_{\text{YZZZ}} \end{bmatrix}$$

Experimental design: striped geometry



motor translation stage:
gap varies from 0.4 to 1 mm

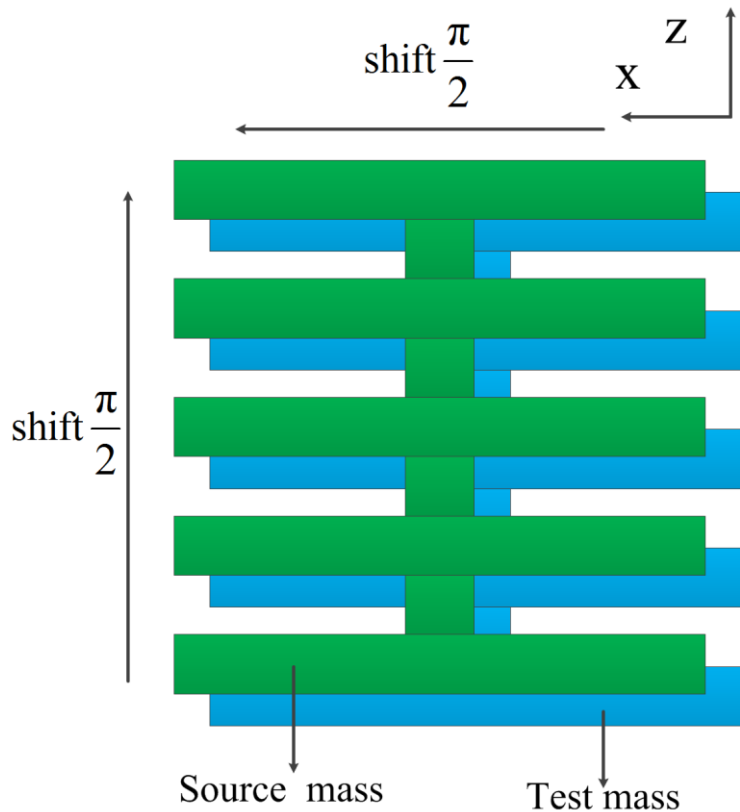


Each strip:
 $1.3 \times 19.8 \times 2.2 \text{ mm}^3$

The feature for test and source masses

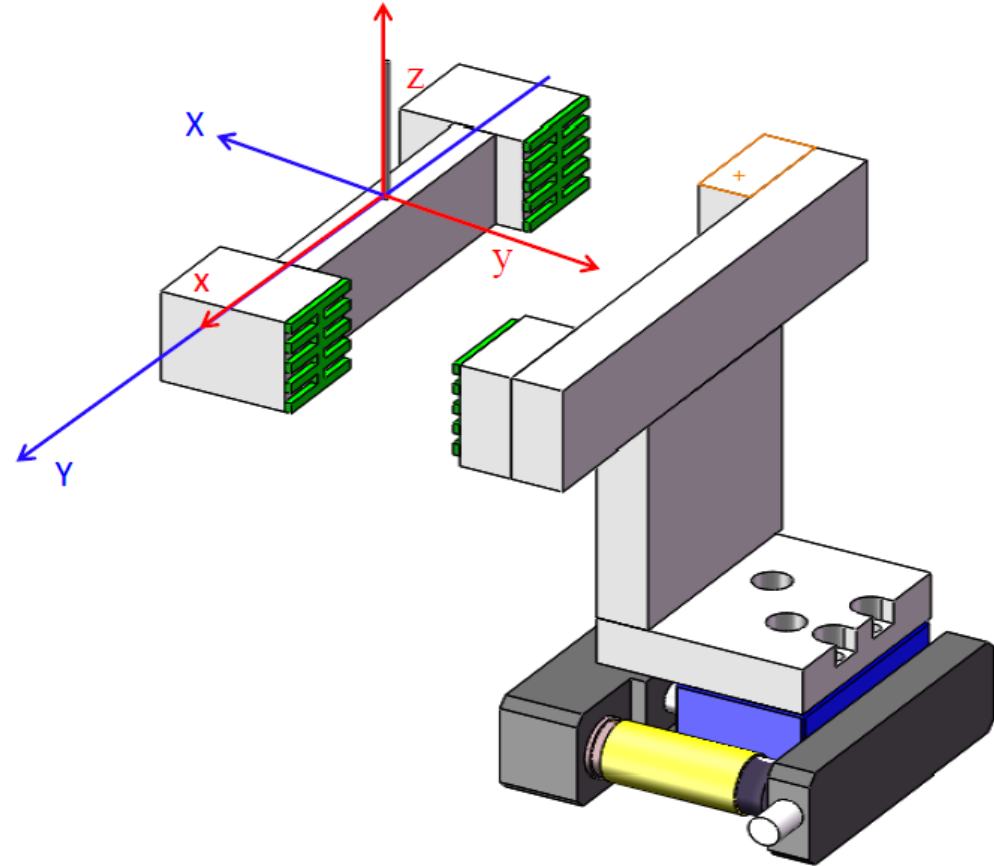


Set horizontal stripe as an example



SME frame

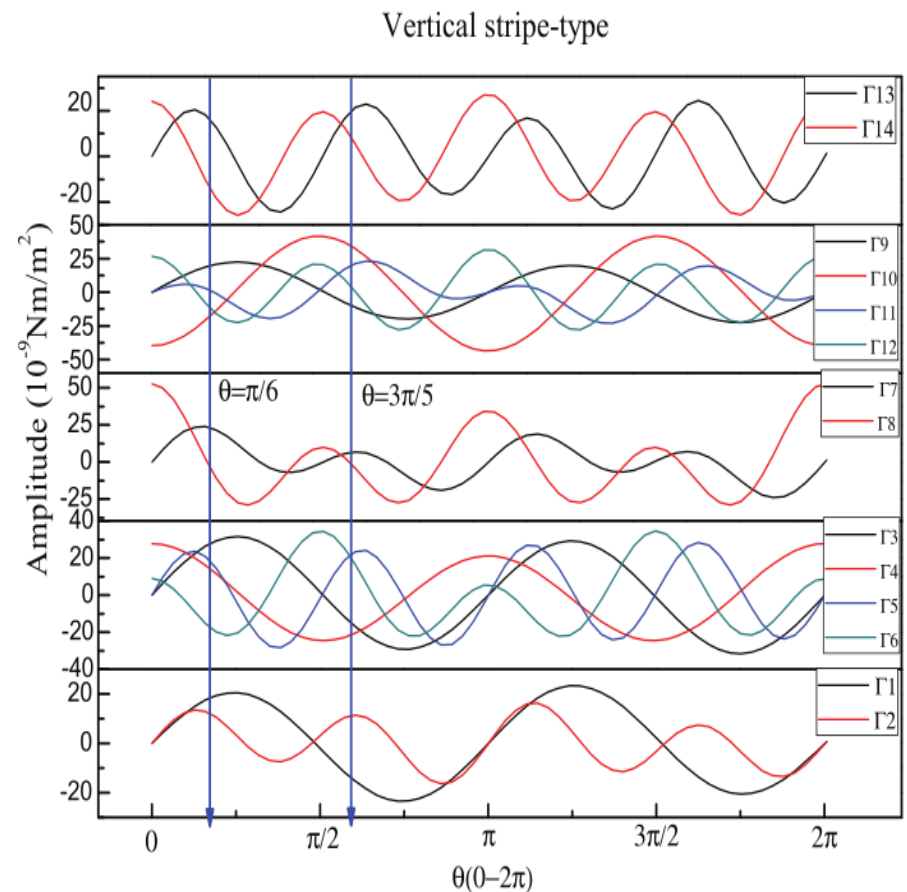
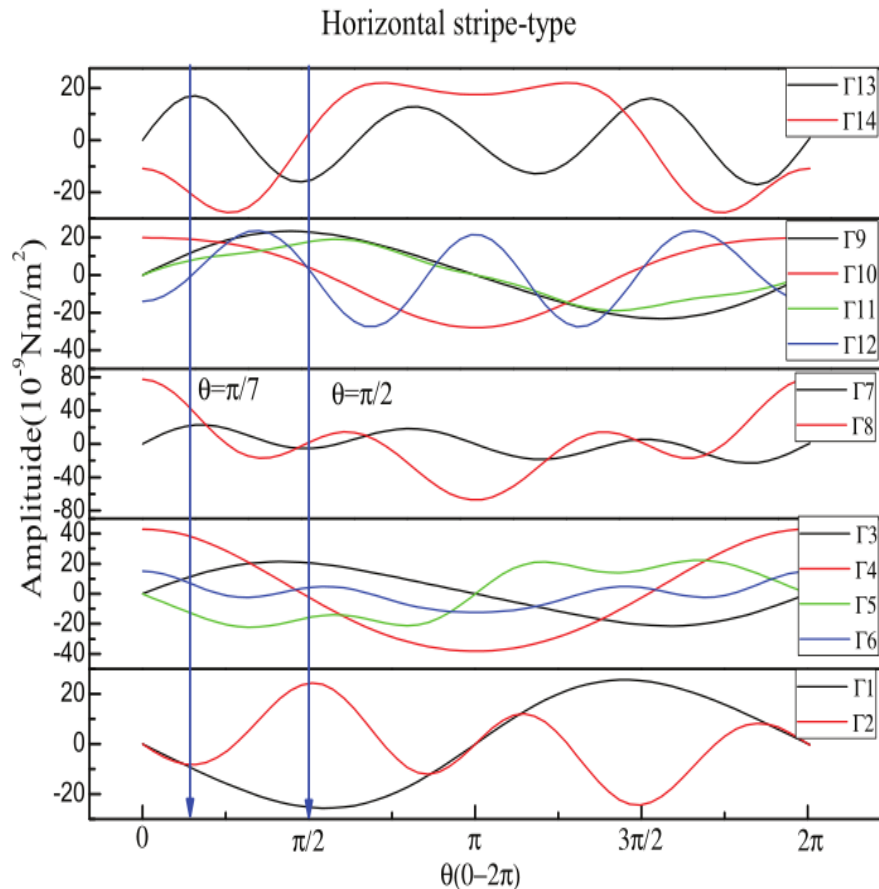
Pendulum frame



shifted up and left half of the width of the strip

Transfer coefficients vary with angle

According to the typical design parameters, we calculate transfer coefficients as functions of angle



Expected signal



Compare to the best current constraint[1]

Assuming $3 \mu\text{m}$ systemic error

Ratio of the total error in the current best constraint to that in our new design

Coefficients	Current constraint (10^{-8}m^2)[21]	Ratio in horizontal stripe-type for $\theta = \pi/7$ and $\pi/2$	Ratio in vertical stripe-type for $\theta = \pi/6$ and $3\pi/5$
$k_{2,0}$	3 ± 23	4	5
$\text{Re } k_{1,1}$	-4 ± 4	16	21
$\text{Im } k_{2,1}$	-2 ± 4	16	21
$\text{Re } k_{2,2}$	0 ± 9	67	73
$\text{Im } k_{2,2}$	1 ± 4	30	32
$k_{4,0}$	4 ± 25	4	4
$\text{Re } k_{4,1}$	3 ± 5	13	14
$\text{Im } k_{4,1}$	1 ± 5	13	14
$\text{Re } k_{2,2}$	0 ± 12	44	92
$\text{Im } k_{2,2}$	2 ± 2	7	15
$\text{Re } k_{4,3}$	0 ± 1	7	7
$\text{Im } k_{4,3}$	1 ± 1	7	7
$\text{Re } k_{4,4}$	2 ± 9	97	49
$\text{Im } k_{4,4}$	2 ± 5	54	27

[1] V. A. Kostelecky. Et al, PLB766,137-143(2017)

Conclusion:



- For the **mSME (d=4)**, the vertical acceleration can be used to test LV. However, the current constraints of LV coefficients are limited by the precision of tidal model.
- For **Quadratic couplings of Riemann curvature** with $d=6$, only the short-range gravity be used to test LV. We suggested an experiment with periodic striped geometry, which may improve the current constraints of LV by about one order of magnitude

Thanks for your attention!